

REPORT

Frontorhiny, a Distinctive Presentation of Frontonasal Dysplasia Caused by Recessive Mutations in the *ALX3* Homeobox Gene

Stephen R.F. Twigg,¹ Sarah L. Versnel,² Gudrun Nürnberg,⁴ Melissa M. Lees,^{6,7} Meenakshi Bhat,⁸ Peter Hammond,⁹ Raoul C.M. Hennekam,^{6,10,13} A. Jeannette M. Hoogeboom,³ Jane A. Hurst,^{14,15} David Johnson,¹⁵ Alexis A. Robinson,¹¹ Peter J. Scambler,⁹ Dianne Gerrelli,¹² Peter Nürnberg,^{4,5,16} Irene M.J. Mathijssen,² and Andrew O.M. Wilkie^{1,14,15,*}

We describe a recessively inherited frontonasal malformation characterized by a distinctive facial appearance, with hypertelorism, wide nasal bridge, short nasal ridge, bifid nasal tip, broad columella, widely separated slit-like nares, long philtrum with prominent bilateral swellings, and midline notch in the upper lip and alveolus. Additional recurrent features present in a minority of individuals have been upper eyelid ptosis and midline dermoid cysts of craniofacial structures. Assuming recessive inheritance, we mapped the locus in three families to chromosome 1 and identified mutations in *ALX3*, which is located at band 1p13.3 and encodes the *aristaleless*-related ALX homeobox 3 transcription factor. In total, we identified seven different homozygous pathogenic mutations in seven families. These mutations comprise missense substitutions at critical positions within the conserved homeodomain as well as nonsense, frameshift, and splice-site mutations, all predicting severe or complete loss of function. Our findings contrast with previous studies of the orthologous murine gene, which showed no phenotype in *Alx3*^{-/-} homozygotes, apparently as a result of functional redundancy with the paralogous *Alx4* gene. We conclude that ALX3 is essential for normal facial development in humans and that deficiency causes a clinically recognizable phenotype, which we term frontorhiny.

Formation of the human face is an exquisitely orchestrated developmental process involving multiple tissue swellings—the frontonasal, medial and lateral nasal, and maxillary and mandibular prominences—derived from the neural crest.¹ During a critical period between 4 and 8 weeks of human fetal development, these processes must undergo cell proliferation and tissue fusion to form the orbital, nasal, and oral structures.^{1,2} Disturbance to this developmental sequence causes frontonasal malformation (FNM), a very heterogeneous group of disorders characterized by combinations of hypertelorism, abnormal nasal configuration, and oral, palatal, or facial clefting, sometimes associated with facial asymmetry, skin tags, ocular or cerebral malformations, widow's peak, and anterior cranium bifidum.^{3–9} Surgical management of FNM often poses substantial challenges.

Most cases of FNM are sporadic, and no cause can be identified. However, disruption to development of the fetal face, caused by transient hypovolemia, haemorrhage into facial tissues, amniotic bands, or teratogens, is suspected to contribute in many cases. In addition, a marked increase in the frequency of monozygotic twinning (with discordance for FNM in the twins) has been noted, suggesting that the twinning process itself may sometimes precipitate the malformation.¹⁰ Genetic causes of FNM are identified in

only a minority of cases; mutations of *EFNB1* (MIM 300035) in craniofrontonasal syndrome (MIM 304110) represent the only consistent association.^{11,12} No mutation of a specific gene(s) has hitherto been identified in isolated FNM.

We initially identified three individuals from two families (subjects 1 and 2 in family 1 and subject 3 in family 2) who shared a similar distinctive facial appearance (Figures 1A and 1C). Subjects 1 and 2 were siblings (male and female, respectively), born to parents who were not known to be related but who originated from adjacent valleys in Morocco; the family history elicited from subject 3, a sporadically affected male from Algeria, was imprecise, but distant parental consanguinity was indicated (Figure 2A). Ethical approval for genetic research and human embryo studies was obtained from the Oxfordshire Research Ethics Committee B (C02.143).

Based on the hypothesis of a shared genetic etiology resulting from inheritance of autosomal-recessive mutations, we undertook a whole-genome linkage analysis by using the GeneChip Human Mapping 250K Sty Array (Affymetrix) and samples from family 1 (subjects 1 and 2, both parents, and three unaffected siblings) and subject 3. We assumed recessive inheritance with full penetrance, a disease allele frequency of 0.0001, and that the parents of affected individuals in families 1 and 2 were each related as

¹Weatherall Institute of Molecular Medicine, University of Oxford, Oxford OX3 9DS, UK; ²Department of Plastic and Reconstructive Surgery, ³Department of Clinical Genetics, Erasmus Medical Center, 3000 CB Rotterdam, The Netherlands; ⁴Cologne Center for Genomics and Institute for Genetics, ⁵Cologne Excellence Cluster on Cellular Stress Responses in Aging-Associated Diseases (CECAD), University of Cologne, D-50674 Cologne, Germany; ⁶Department of Clinical Genetics, ⁷North Thames Cleft Centre, Great Ormond Street Hospital for Children, London WC1N 3JH, UK; ⁸Centre for Human Genetics, Bangalore 560 066, India; ⁹Molecular Medicine Unit, ¹⁰Clinical and Molecular Genetics Unit, ¹¹Neural Development Unit, ¹²Human Developmental Biology Resource, Institute of Child Health, University College London, London WC1N 1EH, UK; ¹³Department of Pediatrics, Academic Medical Centre, University of Amsterdam, 1105 AZ Amsterdam, The Netherlands; ¹⁴Department of Clinical Genetics, ¹⁵Department of Plastic and Reconstructive Surgery, Oxford Radcliffe Hospitals NHS Trust, Oxford OX3 9DU, UK; ¹⁶Center for Molecular Medicine Cologne, University of Cologne, D-50931 Cologne, Germany

*Correspondence: awilkie@hammer.imm.ox.ac.uk

DOI 10.1016/j.ajhg.2009.04.009. ©2009 by The American Society of Human Genetics. All rights reserved.

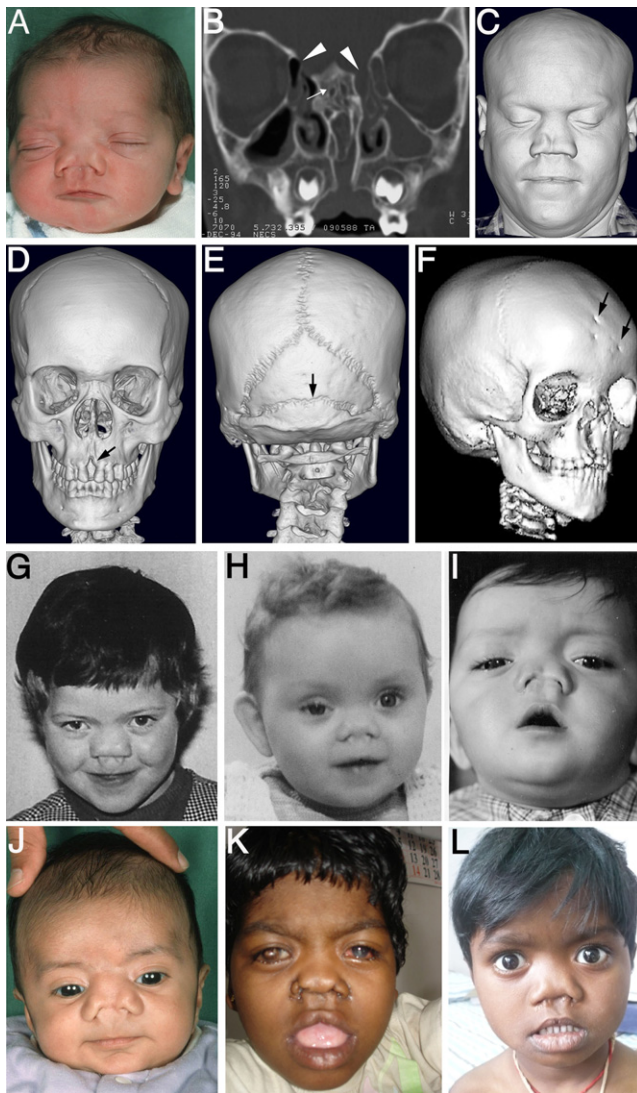


Figure 1. Phenotype of Individuals with Homozygous *ALX3* Mutations

(A and B) Subject 1. Facial appearance at an age of 2 days (A). Coronal CT section at 6 years (B); note broadened dysmorphic ethmoid bone (arrow) and apparent continuities between nasal cavity and brain (arrowheads).

(C–E) Subject 3, pre-operative three-dimensional CT scan at an age of 30 years. Surface scan (C); anterior and posterior views ([D] and [E], respectively), note maxillary diastema (arrow in [D]) and patent sutures with accessory horizontal suture through the occipital bone (arrow in [E]).

(F) Subject 5, three-dimensional CT scan at an age of 5 years. Note maxillary diastema and five paramedian defects in frontal bone, corresponding in position to overlying tissue swellings, probably representing congenital dermoid cysts (arrows).

(G) Subject 6, facial appearance at approximately 6 years.

(H) Subject 7, facial appearance at 1 year.

(I) Subject 8, facial appearance at 2 years.

(J) Subject 9, facial appearance at 2 months.

(K) Subject 10, facial appearance at 4 years. The right eye is pthisical because of an infection.

(L) Subject 11, facial appearance at 2 years.

second cousins. Using ALLEGRO software¹³, we identified two small genomic regions, on chromosomes 1 (maximum heterogeneity LOD [HLOD] score of 4.58) and 12 (maximum HLOD score of 4.52), that were homozygous in affected individuals and consistent with complete linkage (Figure 2B). The chromosome 1 interval, bounded by SNPs rs558370 and rs17671169, which were heterozygous in subject 3, encompassed 653 kb and 15 genes; the chromosome 12 interval, bounded by SNPs rs776195 and rs9988960, which were heterozygous in subjects 1 and 2, encompassed 384 kb and five genes.

The chromosome 1 interval contained a strong candidate gene, *ALX3* ([MIM 606014]; related to the *aristaless* gene in *Drosophila*). This gene, located in band 1p13.3, encodes the ALX homeobox 3 transcription factor, a member of the Paired class of homeodomain proteins.¹⁴ Previous studies of the murine ortholog, *Alx3*, had demonstrated strong expression in the frontonasal mesenchyme.^{15,16} Although the phenotype of *Alx3*^{-/-} mice was normal, a cleft face occurred when these homozygotes were additionally mutant for the paralogous gene *Alx4*.¹⁶ We amplified each of the four exons of *ALX3* (primers and amplification conditions are given in Table S1 in the Supplemental Data) and subjected the products to DNA sequencing and confirmatory restriction digests. This showed that subjects 1 and 2 were homozygous for a nucleotide substitution (595-2A > T) in the canonical 3' splice acceptor sequence of intron 2; subject 3 was homozygous for an exon 3 nucleotide substitution (608A > G) encoding an N203S missense mutation at a very highly conserved asparagine residue in helix III of the homeodomain that directly contacts DNA (Figure 3A, Table 1).¹⁷

We extended the analysis to additional patients with FNM (Figure 2A). Lees et al.¹⁸ reported two siblings from a sibship of seven (subjects 4 and 5, family 3) with a similar phenotype; analysis of samples from this family by means of the GeneChip Human Mapping 10K Xba Array (Affymetrix) indicated that subjects 4 and 5 were homozygous for a 15.9 Mb region on the short arm of chromosome 1; this region was bounded by heterozygous SNPs rs10493874 and rs3908929 and included the *ALX3* gene (data not shown). Both affected individuals were homozygous for the *ALX3* mutation 502C > G, encoding a L168V substitution in the homeodomain. We identified four different mutations of *ALX3* (all homozygous) in four previously unpublished families (subjects 6–11, families 4–7) (Figure 3A, Table 1). We either confirmed that the mutations were heterozygous in both parental samples by using restriction digests (Table S1 details those cases in which mutant oligonucleotide primers were employed in these digests) or used multiplex ligation-dependent probe amplification (MLPA) to demonstrate that the mutant allele was present in two copies in affected individuals (MLPA primers and conditions are listed in Table S2). Although the second linkage signal initially observed on chromosome 12 raises a possible requirement for the digenic inheritance of mutations, both the high rate of

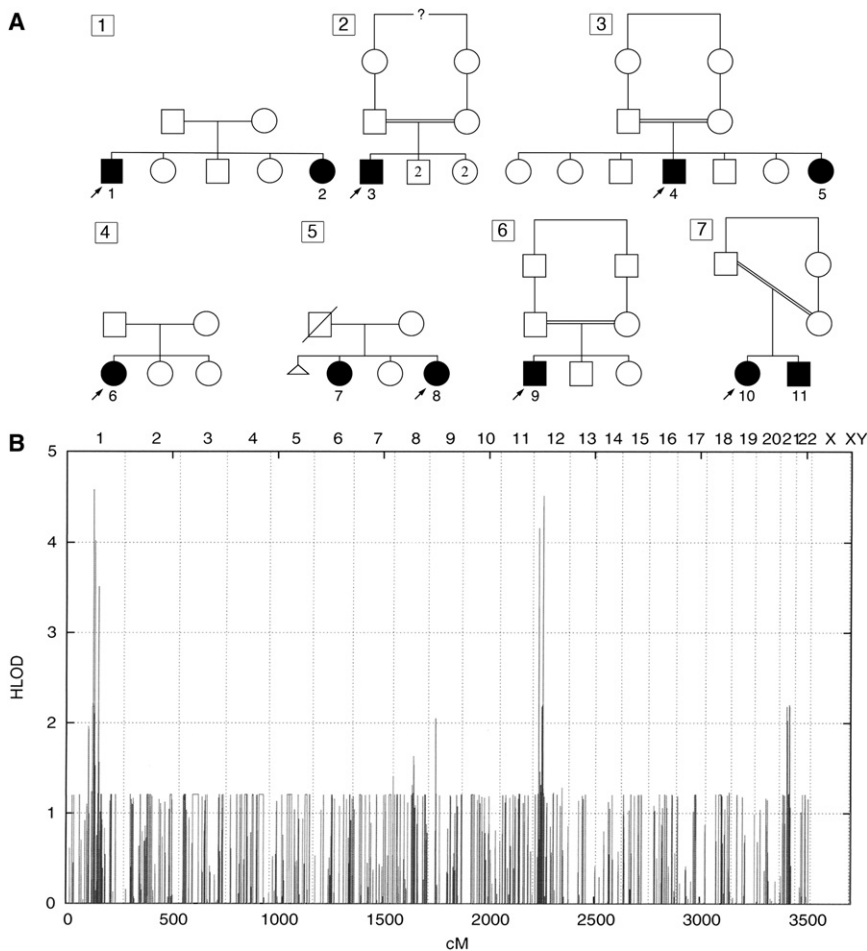


Figure 2. Pedigrees and Disease Localization

(A) Pedigrees of families 1–7. (B) Whole-genome linkage analysis of families 1 and 2.

DNA binding.²² The R183W substitution occurs at position 31 in helix II; this arginine residue is highly conserved in the Paired class and several other classes of homeodomain,²¹ and its formation of a buried salt bridge with glutamate at position 42 contributes to the structural integrity of the homeodomain. An equivalent mutation (R298W) was previously described in the homeodomain of HOXD13 (MIM 142989); in vitro studies of several different substitutions of the position 31 arginine have shown severe or complete loss of DNA binding.²³ The 586C > T (R196W) substitution occurs at position 44 in helix III. Although not very highly conserved across homeodomains as a whole, this arginine residue is a common feature in the Paired class¹⁴ and makes contact with DNA.²⁴ A mutation (R141G) at the equivalent position of the Paired class

homeodomain of PHOX2B (MIM 603851) was shown to abolish DNA binding.²⁵ Finally, the N203S substitution occurs at the position 51 asparagine; this residue directly contacts an adenine base in bound DNA and is one of the most highly conserved residues in the entire homeodomain.¹⁷ Mutations of this asparagine to serine in several different homeodomain-containing proteins resulted in severely reduced DNA binding.²⁶ None of the mutations that we identified was present in the DNA sequences of a minimum of 226 unrelated control chromosomes of north European origin.

phenotype recurrence in siblings (Figure 2A) and the absence of unaffected siblings homozygous for *ALX3* mutations (Figure 3A) argue against this; it is more likely that the chromosome 12 signal represents a type I error. The genotyping identified 18 individuals heterozygous for an *ALX3* mutation (Figure 3A), and none of these exhibited unusual facial features suggestive of a manifesting carrier state.

The mutations are all consistent with severe or complete loss of DNA binding by the mutant *ALX3* protein. The nonsense (543T > A; Y181X), frameshift (578_581 delCTGA; T193RfsX137), and acceptor splice-site (595-2A > T) mutations are predicted to lead to loss of the DNA-binding helix III of the homeodomain and thus complete loss of function (Figure 3B). The other mutations are missense substitutions that occur at some of the most highly conserved residues within the 60 amino acid DNA-binding homeodomain; multiple missense mutations causing loss of function have been reported previously at the equivalent residues of other homeodomain transcription factors.^{19,20} The L168V substitution occurs at position 16 in helix I of the homeodomain, This leucine residue, which is conserved in the Paired class and several other classes of human homeodomains,²¹ is buried in the hydrophobic core²⁰, and an L132V substitution at the equivalent position of the SHOX (MIM 312865) homeodomain showed loss of dimerization and very weak

We used dense surface modeling²⁷ to analyze objectively the abnormal facial morphology in subjects 3, 4, and 5. Although this consistently demonstrated maximal tissue deficiency in the midfacial region around the nose and philtrum, the degree of hypertelorism and mid-face hypoplasia was much more marked in subjects 5 and 3 (not illustrated) compared with subject 4 (Figure 4). In contrast, subject 4 showed significant upward displacement of the nose and, to a lesser extent, of the supraorbital region (Figure 4; these differences are also demonstrated in the dynamic morphs in Movies S1 and S2). These findings and the clinical features are consistent with embryonic tissue disturbance predominantly affecting the frontonasal and medial nasal prominences;¹ the relatively high prevalence of congenital dermoid cysts is consistent with

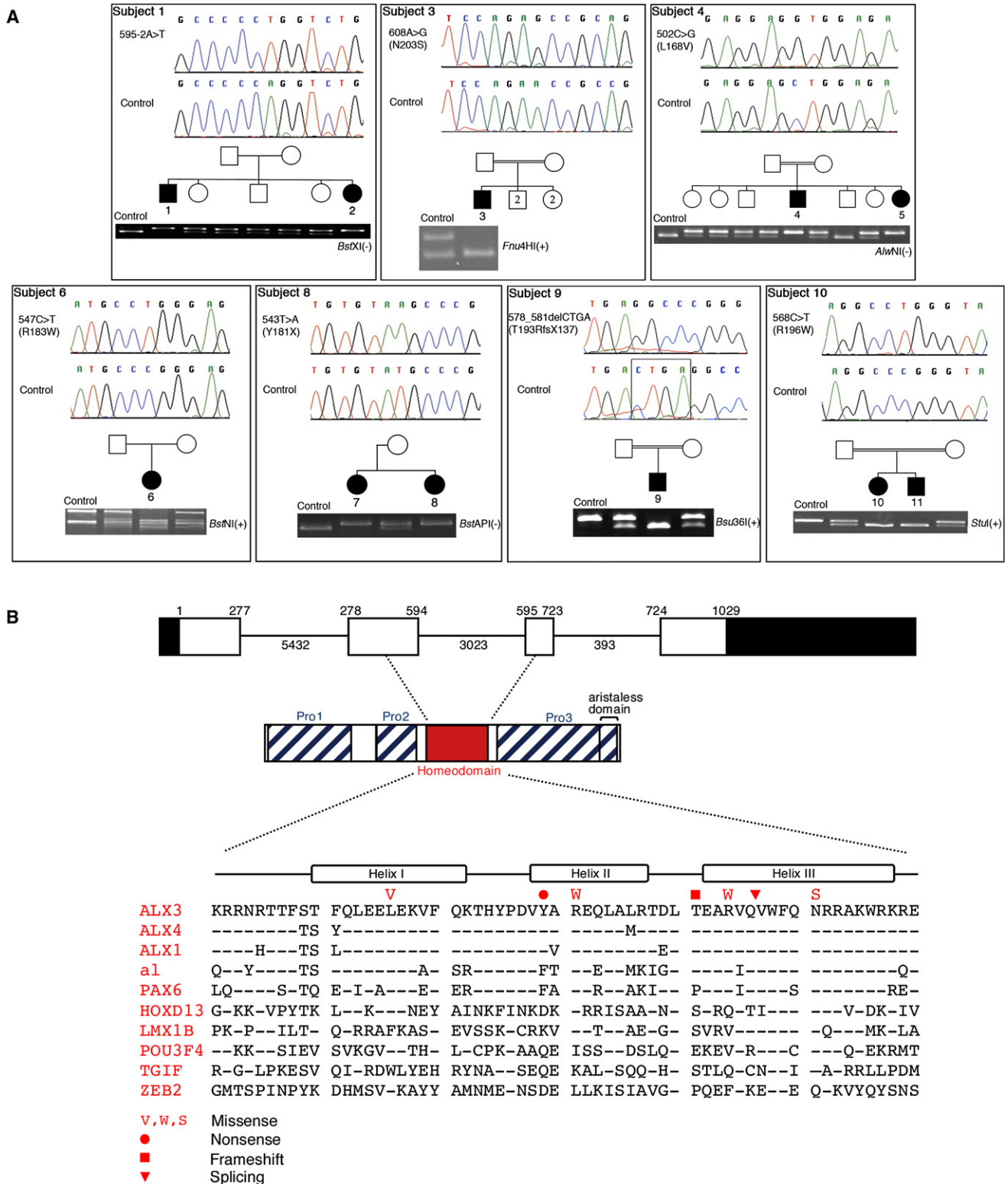


Figure 3. Mutations Identified in the ALX3 Gene

(A) DNA-sequence chromatograms (above) and confirmatory restriction digests (below) of the seven different mutations identified in this work.

(B) Cartoon showing (top) genomic organization of ALX3 (numbers above boxes indicate cDNA numbering at exon boundaries; numbers below lines indicate intron sizes) and (middle) domain organization of the protein.³⁹ At bottom is shown the position of individual mutations within the homeodomain of ALX3, compared with other proteins from the Paired class (human ALX4 and ALX1, *Drosophila* al, human PAX6) and representative examples of increasingly divergent human homeodomain proteins from the other major classes (HOXD13, ANTP class; LMX1B, LIM class; POU3F4, POU class; TGIF, TALE class; and ZEB2, ZF class).²¹ Dashes indicate residues conserved with respect to human ALX3.

Table 1. Mutation Details and Clinical Features of Subjects with *ALX3* Mutation

Sample ID	Subject	Family	Sex ^a	Country of Origin	Reported Consanguinity ^a	Exon (Intron) Number	Nucleotide Change (All Homozygous)	Predicted Amino Acid Change	Additional Clinical Features ^a
4143	1	1	M	Morocco	N	(2)	595-2A > T	*	Cleft palate, bony defect of anterior cranial fossa with recurrent meningitis
4144	2	1	F	Morocco	N	(2)	595-2A > T	*	Cleft palate, convergent squint
4150	3	2	M	Algeria	Y	3	608A > G	N203S	Accessory suture in occipital bone
4179	4	3	M	Ireland	Y	2	502C > G	L168V	R eyelid ptosis, strabismus, choanal stenosis, midline philtral pit connected to dermoid cyst
4180	5	3	F	Ireland	Y	2	502C > G	L168V	Lipoma of corpus callosum, paramedian frontal bone cysts, midline philtral pit connected to dermoid cyst, midline cleft of upper lip
4254	6	4	F	Netherlands	N	2	547C > T	R183W	R iris coloboma, orbital dystopia
4252	7	5	F	Netherlands	N	2	543T > A	Y181X	R eyelid ptosis, scoliosis
4251	8	5	F	Netherlands	N	2	543T > A	Y181X	R eyelid ptosis, lumbar lordosis
4295	9	6	M	Turkey	Y	2	578_581 delCTGA	T193RfsX137	-
4291	10	7	F	India	Y	2	586C > T	R196W	Rugosity behind external ears, notched alae nasae
4292	11	7	M	India	Y	2	586C > T	R196W	Bifid tongue, rugosity behind external ears

* Splice-site mutation.

^a Abbreviations: F, female; M, male; N, no; R, right; and Y, yes.

disturbance of fusion of the frontal and medial nasal prominences and resulting buried ectodermal components.

To explore the phenotypic range of *ALX3* mutations, we undertook DNA sequencing of *ALX3* in 14 additional unrelated individuals with various FNMs. These included one individual who was reported to have possible Pai syndrome (MIM 155145)²⁸, one with oculoauriculofrontonasal syndrome (MIM 601452)²⁹, three with acromelic frontonasal dysostosis (MIM 603671)^{30,31}, and nine with miscellaneous combinations of hypertelorism, facial tags, and facial clefting⁶; none of these individuals exhibited *ALX3* mutations. DNA sequencing of *ALX3* in 93 patients with nonsyndromic cleft lip and/or palate also gave normal results.

We conclude that the phenotypic range from homozygous loss-of-function of *ALX3* appears to be narrow and is characterized by the distinctive facial appearance shown in Figure 1; no genotype-phenotype correlation is apparent. The major features characterizing this disorder are hypertelorism, wide nasal bridge, short nasal ridge, splayed nasal

bones with bifid nasal tip, broad columella that attaches to the face above the alae, widely separated slit-like nares, long philtrum, prominent philtral ridges that sometimes have additional bilateral swellings that run into the nares, and midline notch in the upper lip and alveolus. Additional features present in some patients were upper eyelid ptosis (three subjects), inclusion dermoids of craniofacial structures, philtral pits or rugose folding behind the ears (two subjects each), and iris coloboma, strabismus, and lipoma of the corpus callosum (one subject each). Review of skull radiographs or computed tomographic (CT) scans of five subjects (1, 3, 5, 6, and 8) did not show craniosynostosis; an accessory suture in the occipital bone was present in subject 3 (Figure 1E). Of clinical significance, subject 1 had six episodes of pneumococcal meningitis, which were associated with rhinorrhea of cerebrospinal fluid and were found to be related to multiple defects in the cribriform plate of the ethmoid bone (Figure 1B); subject 5 had several subcutaneous forehead swellings associated with

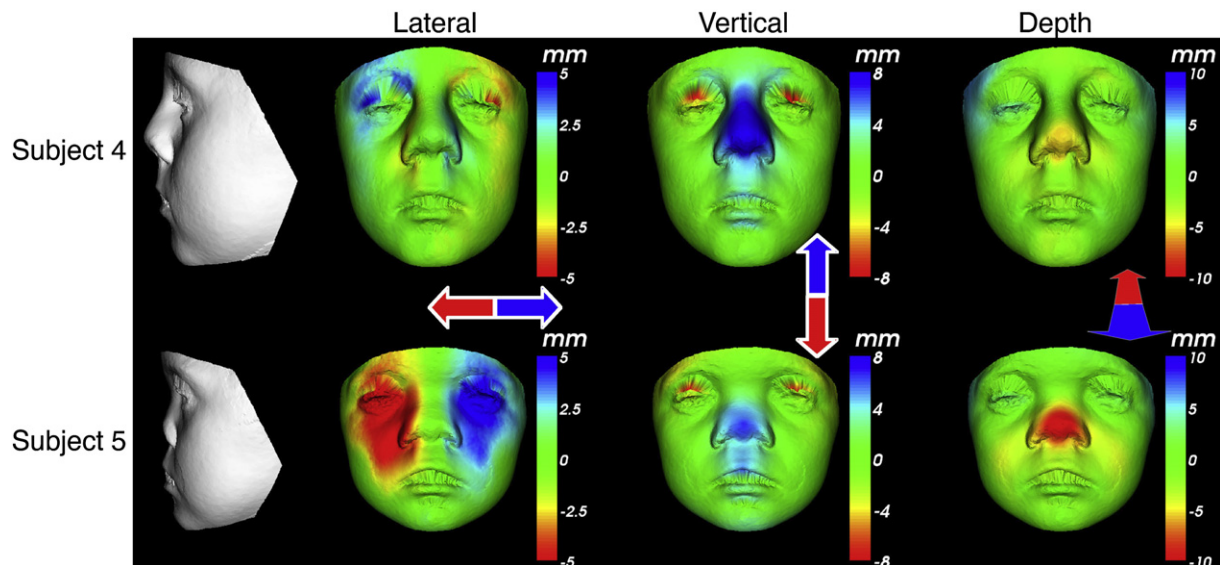


Figure 4. Dense Surface-Modeling Analysis of Subjects 4 and 5

Subject 4 (above, postoperative after insertion of nasal silastic strut, aged 10 years) and subject 5 (below, prior to nasal augmentation, aged 5 years) were compared, in terms of lateral, vertical and depth displacement, to average faces of appropriately age- and sex-matched controls. Green regions coincide on both patient and average face. Red regions indicate displacement of parts of the subject's face in a direction more rightward, downward, or inward, and blue regions indicate displacement in a direction more leftward, upward, or outward. Color coding is shown on the accompanying scales. Note that subject 5 has greater hypertelorism and midfacial hypoplasia than subject 4.

paramedian foraminae in the frontal bone, suggestive of dermoids (Figure 1F). Growth and development have been normal in all subjects, but most have required surgical procedures for improved appearance and function. These have included multiple nasal reconstructions (involving 12 and 13 separate procedures, respectively, in subjects 8 and 7), ptosis correction (subjects 6, 7, and 8), strabismus correction (subject 2), excision of dermoid cysts (subjects 4 and 5), cleft palate repair (subjects 1 and 2), midline cleft-lip repair (subject 5), Le Fort I advancement of maxilla (subjects 1 and 6), Le Fort III advancement and medialization of orbits (subjects 1 and 7), and repair of the anterior cranial-base defect and reconstruction of the nasal airway (subject 1).

The craniofacial phenotype associated with *ALX3* mutations seems to represent a poorly recognized clinical entity. Subjects 4 and 5 were previously described¹⁸, but similar patients are not illustrated in any of the literature classifying the diverse presentations of FNM.^{3–9} Lees et al.¹⁸ drew attention to the resemblance of the affected siblings in their report to a unique family with a phenotype named craniorhiny (MIM 123050).³² Although it has not been possible to trace the originally reported craniorhiny family for genetic analysis, three considerations argue that the *ALX3*-mutation-positive subjects have a different condition. First, there is differing facial morphology in craniorhiny, in which nasal outgrowth is much better preserved; second, craniosynostosis was observed in several individuals with craniorhiny but is not documented in association with *ALX3* mutations; third, vertical transmission suggesting dominant inheritance was described in craniorhiny,³² whereas *ALX3* mutations exhibit recessive inheritance. The nasal

appearance in our subjects is reminiscent to the family reported by Fryburg et al. (MIM 305645)³³, but the phenotype in that family also showed vertical transmission. A possible match is the proband in the report by Toriello et al. (MIM 164000)³⁴; this individual shows a similar nasal appearance to subject 7, was the offspring of a consanguineous union, and had white Dutch ancestry, like subjects 6–8 in our series. Otherwise, our attempts to identify patients in the literature who match those reported here have, surprisingly, failed. Hence, to our knowledge this is a new genetic syndrome of FNM, for which we suggest the name frontorhiny. Although acknowledging the mixed etymological origin of this term, we believe that it best encompasses the characteristic combination of frontal and nasal malformations in affected individuals (Figures 1 and 4) and the clinical overlap with previously described craniorhiny.^{18,32}

As previously noted, *Alx3*^{-/-} mice are phenotypically normal, indicating a greater requirement for *ALX3* in development of the frontonasal region in the human than in the mouse. However, both *Alx3* and the paralogous gene *Alx4* are expressed in the frontonasal mesenchyme at embryonic days (E) 9.5–11.5 in the mouse, and mice mutant for three alleles of these two genes (either *Alx3*^{-/-}; *Alx4*^{+/*Alst-J*} or *Alx3*^{+/-}; *Alx4*^{*lst-J*/*lst-J*}) exhibit facial clefting.¹⁶ This was correlated with increased apoptosis of the developing frontonasal mesenchyme at E10.0, suggesting that the primary defect in combined *Alx3* and *Alx4* deficiency is failure to support normal cell survival in part of the frontonasal process during a critical period of development. In humans, heterozygous mutations of *ALX4* (MIM 605420) cause parietal foramina (PFM2 [MIM 609597]).^{35,36} We

confirmed by DNA sequencing and MLPA (Tables S1 and S2) that there were no mutations or deletions of either *ALX4* or the paralogous *ALX1* gene ([MIM 601527]; previously termed *CART1*)³⁷ in the *ALX3*-mutated individuals.

We attempted to compare the expression patterns of *ALX3* and *ALX4* in the frontonasal prominences of human embryos. We were unable to obtain signals above background for *ALX3*, but we observed apparent expression of *ALX4* in the medial nasal processes of an embryo at Carnegie stage 16, equivalent to ~37 days post fertilization (Figure S1). This excludes a mechanism whereby the abnormal frontonasal phenotype in *ALX3*-deficient humans, compared to mice, is simply attributable to a complete lack of *ALX4* expression in the medial nasal process of the human embryo and the resulting absolute dependence on *ALX3* expression. Our analysis does not, however, exclude a more subtle effect involving the relative timing and levels of *ALX3* and *ALX4* in the developing facial structures.

In conclusion, we have identified a recurrent pattern of FNM that is caused by recessive mutations in the homeobox gene *ALX3*. This is the first isolated FNM shown to have a specific genetic etiology, as opposed to arising from a prenatal developmental insult. It is important to recognize this disorder, for which we propose the term frontorhiny, because of its specific implications for diagnostic testing and genetic counselling and association with congenital dermoid cysts with the potential for transcranial extension. Our work also illustrates the power of homozygosity mapping to identify rare recessive disease genes from very few samples of uncertain consanguineous origin.³⁸

Supplemental Data

Supplemental data comprise one figure, two tables, and two movies and can be found with this article online at <http://www.ajhg.org/>.

Acknowledgments

We are very grateful to M. Cunningham, A. Hing, R. Newbury-Ecob, S. Robertson, and S. Smithson for additional patient samples analyzed in this study, to C. Becker for SNP chip processing, to K. Clarke for DNA sequencing, to M. van den Elzen for help with data collection, to P. Stanier for collaboration on analysis of cleft lip and palate samples, and to N. Akarsu for discussions. Human embryonic material was provided by the MRC/Wellcome Trust-funded Human Developmental Biology Resource. This work was supported by the Wellcome Trust (Programme Grant to A.O.M.W.).

Received: March 9, 2009

Revised: April 3, 2009

Accepted: April 14, 2009

Published online: April 30, 2009

Web Resources

Accession numbers and URLs for data presented herein are as follows:

dbSNP, <http://www.ncbi.nlm.nih.gov/SNP/>

GenBank, <http://www.ncbi.nlm.nih.gov/Genbank/index.html> (for human *ALX3* cDNA reference sequence, accession number NM_006492.2)

MRC-Holland, <http://www.mrc-holland.com/WebForms/WebFormMain.aspx?Tag=fNPBLedDVp38p/CxU2h0mQ> (for information on MLPA reagents and methods)

Online Mendelian Inheritance in Man (OMIM), <http://www.ncbi.nlm.nih.gov/Omim>

References

1. Moore, K.L., and Persaud, T.V.N. (2007). *The Developing Human* (Philadelphia: W.B. Saunders).
2. Yoon, H., Chung, I.S., Seol, E.Y., Park, B.Y., and Park, H.W. (2000). Development of the lip and palate in staged human embryos and early fetuses. *Yonsei Med. J.* 41, 477–484.
3. DeMyer, W. (1967). The median cleft face syndrome. Differential diagnosis of cranium bifidum occultum, hypertelorism, and median cleft nose, lip, and palate. *Neurology* 17, 961–971.
4. Sedano, H.O., Cohen, M.M. Jr., Jirasek, J., and Gorlin, R.J. (1970). Frontonasal dysplasia. *J. Pediatr.* 76, 906–913.
5. Sedano, H.O., and Gorlin, R.J. (1988). Frontonasal malformation as a field defect and in syndromic associations. *Oral Surg. Oral Med. Oral Pathol.* 65, 704–710.
6. van der Meulen, J.C.H., and Vaandrager, J.M. (1989). Facial clefts. *World J. Surg.* 13, 373–383.
7. Guion-Almeida, M.L., Richieri-Costa, A., Saavedra, D., and Cohen, M.M. Jr. (1996). Frontonasal dysplasia: Analysis of 21 cases and literature review. *Int. J. Oral Maxillofac. Surg.* 25, 91–97.
8. Tan, S.T., and Mulliken, J.B. (1997). Hypertelorism: Nosologic analysis of 90 patients. *Plast. Reconstr. Surg.* 99, 317–327.
9. Losee, J.E., Kirschner, R.E., Whitaker, L.A., and Bartlett, S.P. (2004). Congenital nasal anomalies: A classification scheme. *Plast. Reconstr. Surg.* 113, 676–689.
10. Mohammed, S.N., Swan, M.C., Wall, S.A., and Wilkie, A.O.M. (2004). Monozygotic twins discordant for frontonasal malformation. *Am. J. Med. Genet.* 130A, 384–388.
11. Twigg, S.R.F., Kan, R., Babbs, C., Bochukova, E.G., Robertson, S.P., Wall, S.A., Morriss-Kay, G.M., and Wilkie, A.O.M. (2004). Mutations of ephrin-B1 (*EFNB1*), a marker of tissue boundary formation, cause craniofrontonasal syndrome. *Proc. Natl. Acad. Sci. USA* 101, 8652–8657.
12. Wieland, I., Jakubiczka, S., Muschke, P., Cohen, M., Thiele, H., Gerlach, K.L., Adams, R.H., and Wieacker, P. (2004). Mutations of the ephrin-B1 gene cause craniofrontonasal syndrome. *Am. J. Hum. Genet.* 74, 1209–1215.
13. Gudbjartsson, D.F., Jonasson, K., Frigge, M.L., and Kong, A. (2000). Allegro, a new computer program for multipoint linkage analysis. *Nat. Genet.* 25, 12–13.
14. Galliot, B., de Vargas, C., and Miller, D. (1999). Evolution of homeobox genes: Q₅₀ Paired-like genes founded the Paired class. *Dev. Genes Evol.* 209, 186–197.
15. Ten Berge, D., Brouwer, A., El Bahi, S., Guénet, J.-L., Robert, B., and Meijlink, F. (1998). Mouse *Alx3*: An *aristalless*-like homeobox gene expressed during embryogenesis in ectomesenchyme and lateral plate mesoderm. *Dev. Biol.* 199, 11–25.
16. Beverdam, A., Brouwer, A., Reijnen, M., Korving, J., and Meijlink, F. (2001). Severe nasal clefting and abnormal embryonic apoptosis in *Alx3/Alx4* double mutant mice. *Development* 128, 3975–3986.

17. Noyes, M.B., Christensen, R.G., Wakabayashi, A., Stormo, G.D., Brodsky, M.H., and Wolfe, S.A. (2008). Analysis of homeodomain specificities allows the family-wide prediction of preferred recognition sites. *Cell* 133, 1277–1289.
18. Lees, M.M., Kangesu, L., Hall, P., and Hennekam, R.C.M. (2007). Two siblings with an unusual nasal malformation: Further instances of craniorhiny? *Am. J. Med. Genet.* 143A, 3290–3294.
19. D'Elia, A.V., Tell, G., Paron, I., Pellizzari, L., Lonigro, R., and Damante, G. (2001). Missense mutations of human homeoboxes: A review. *Hum. Mutat.* 18, 361–374.
20. Chi, Y.-I. (2005). Homeodomain revisited: A lesson from disease-causing mutations. *Hum. Genet.* 116, 433–444.
21. Holland, P.W.H., Booth, H.A.F., and Bruford, E.A. (2007). Classification and nomenclature of all human homeobox genes. *BMC Biol.* 5, 47.
22. Schneider, K.U., Marchini, A., Sabherwal, N., Röth, R., Niesler, B., Marttila, T., Blaschke, R.J., Lawson, M., Dumic, M., and Rappold, G. (2005). Alteration of DNA binding, dimerization, and nuclear translocation of SHOX homeodomain mutations identified in idiopathic short stature and Leri-Weill dyschondrosteosis. *Hum. Mutat.* 26, 44–52.
23. Debeer, P., Bacchelli, C., Scambler, P.J., De Smet, L., Fryns, J.-P., and Goodman, F.R. (2002). Severe digital abnormalities in a patient heterozygous for both a novel missense mutation in *HOXD13* and a polyalanine tract expansion in *HOXA13*. *J. Med. Genet.* 39, 852–856.
24. Bruun, J.-A., Thomassen, E.I.S., Kristiansen, K., Tylden, G., Holm, T., Mikkola, I., Bjørkøy, G., and Johansen, T. (2005). The third helix of the homeodomain of paired class homeodomain proteins acts as a recognition helix both for DNA and protein interactions. *Nucleic Acids Res.* 33, 2661–2675.
25. Trochet, D., Hong, S.J., Lim, J.K., Brunet, J.-F., Munnich, A., Kim, K.-S., Lyonnet, S., Goridis, C., and Amiel, J. (2005). Molecular consequences of PHOX2B missense, frameshift and alanine expansion mutations leading to autonomic dysfunction. *Hum. Mol. Genet.* 14, 3697–3708.
26. Shanmugam, K., Green, N.C., Rambaldi, I., Saragovi, H.U., and Featherstone, M.S. (1999). PBX and MEIS as non-DNA-binding partners in trimeric complexes with HOX proteins. *Mol. Cell. Biol.* 19, 7577–7588.
27. Hammond, P., Hutton, T.J., Allanson, J., Buxton, B., Campbell, L., Clayton-Smith, J., Donnai, D., Karmiloff-Smith, A., Metcalfe, K., Murphy, K.C., et al. (2005). Discriminating power of localised 3D facial morphology. *Am. J. Hum. Genet.* 77, 999–1010.
28. Lees, M.M., Connelly, F., Kangesu, L., Sommerlad, B., and Barnicoat, A. (2006). Midline cleft lip and nasal dermoids over five generations: A distinct entity or autosomal dominant Pai syndrome? *Clin. Dysmorphol.* 15, 155–159.
29. Gabbett, M.T., Robertson, S.P., Broadbent, R., Aftimos, S., Sachdev, R., and Nezarati, M.M. (2008). Characterizing the oculoauriculofrontonasal syndrome. *Clin. Dysmorphol.* 17, 79–85.
30. Slaney, S.F., Goodman, F.R., Eilers-Walsman, B.L.C., Hall, B.D., Williams, D.K., Young, I.D., Hayward, R.D., Jones, B.M., Christianson, A.L., and Winter, R.M. (1999). Acromelic frontonasal dysostosis. *Am. J. Med. Genet.* 83, 109–116.
31. Hing, A.V., Syed, N., and Cunningham, M.L. (2004). Familial acromelic frontonasal dysostosis: Autosomal dominant inheritance with reduced penetrance. *Am. J. Med. Genet.* 128A, 374–382.
32. Mindikoğlu, A.N., Erginel, A., and Cenani, A. (1991). An unknown syndrome of nose deformity, oxycephaly, aplasia of the nasolacrimal ducts, and symmetrical cyst formation on the upper lip in siblings: Craniorhiny. *Plast. Reconstr. Surg.* 88, 699–702.
33. Fryburg, J.S., Persing, J.A., and Lin, K.Y. (1993). Frontonasal dysplasia in two successive generations. *Am. J. Med. Genet.* 46, 712–714.
34. Toriello, H.V., Higgins, J.V., Walen, A., and Waterman, D.F. (1985). Familial occurrence of a developmental defect of the medial nasal processes. *Am. J. Med. Genet.* 21, 131–135.
35. Wuyts, W., Cleiren, E., Homfray, T., Rasore-Quartino, A., Vanhoenacker, F., and Van Hul, W. (2000). The *ALX4* homeobox gene is mutated in patients with ossification defects of the skull (foramina parietalia permagna, OMIM 168500). *J. Med. Genet.* 37, 916–920.
36. Mavrogiannis, L.A., Antonopoulou, I., Baxová, A., Kutílek, S., Kim, C.A., Sugayama, S.M., Salamanca, A., Wall, S.A., Morriss-Kay, G.M., and Wilkie, A.O.M. (2001). Haploinsufficiency of the human homeobox gene *ALX4* causes skull ossification defects. *Nat. Genet.* 27, 17–18.
37. Qu, S., Tucker, S.C., Zhao, Q., deCrombrugge, B., and Wisdom, R. (1999). Physical and genetic interactions between *Alx4* and *Cart1*. *Development* 126, 359–369.
38. Hildebrandt, F., Heeringa, S.F., Rüschenhoff, F., Attanasio, M., Nürnberg, G., Becker, C., Seelow, D., Huebner, N., Chernin, G., Vlangos, C.N., et al. (2009). A systematic approach to mapping recessive disease genes in individuals from outbred populations. *PLoS Genetics* 5, e1000353.
39. Pérez-Villamil, B., Mirasierra, M., and Vallejo, M. (2004). The homeoprotein *Alx3* contains discrete functional domains and exhibits cell-specific and selective monomeric binding and transactivation. *J. Biol. Chem.* 279, 38062–38071.